

Scientific paper

Four Different Crystalline Products from One Reaction: Unexpected Diversity of Products of the CuCl_2 Reaction with *N*-(2-Pyridyl)thiourea

Sara Tomšič, Janez Košmrlj and Andrej Pevec*

Faculty of Chemistry and Chemical Technology, University of Ljubljana, Večna pot 113, 1000 Ljubljana, Slovenia

* Corresponding author: E-mail: andrej.pevec@fkkt.uni-lj.si

Received: 07-10-2020

Abstract

The reaction of *N*-(2-pyridyl)thiourea with CuCl_2 in methanol yields four different crystalline products: yellow dimeric complex, $[\text{Cu}_2\text{Cl}_2(\mu\text{-Cl})_2(\text{L})_2]$ (**1**), red polymeric complex, $[\text{Cu}_3\text{Cl}_8\text{L}_2]_n$ (**2**), orange crystalline product with ionic structure, $\text{L}_2[\text{CuCl}_4]$ (**3**), and colourless ionic compound LCl (**4**), where **L** = 2-amino-[1,2,4]thiadiazolo[2,3-*a*]pyridin-4-ium cation as a result of oxidative cyclization of *N*-(2-pyridyl)thiourea. The crystal structures of all these crystalline products have been determined by single-crystal X-ray diffraction analysis. Compound **1** involves a copper(I) ion while in **2** and **3** the copper centre is in the divalent state. ^1H NMR spectra for compounds **1–3** are identical and confirm deprotonated thioamide groups of *N*-(2-pyridyl)thiourea and the formation of a thiadiazolopyridinium cation in solution. The hydrogen bonding and π - π stacking interactions were investigated in the solid state. In addition, all crystalline products **1–4** exhibit also S...Cl bonding interactions which consolidate the complexes into networks. The X-ray diffraction analyses indicate the absence of other crystalline phases in the crude reaction mixture.

Keywords: Cu(II) complex; Cu(I) complex; oxidative cyclization; crystal structure, thiourea

1. Introduction

Thiourea and its derivatives are readily oxidized in both aqueous and non-aqueous solutions by several oxidizing agents including bromine, iodine and copper(II) ions.¹ The reaction of thiourea and its derivatives with copper(II) salts in solution results in a reduction of Cu(II) ions into Cu(I) and the formation of many different stable polynuclear products.^{2–12} The chemistry of thioureas in copper-ion containing solutions is complex due to a variable and frequently uncertain nature of the redox processes involved. A number of copper(I) and even copper(II) complexes have been obtained with different molecular structures.¹³ The oxidation and redox kinetics in copper(II) – thioureas systems have been investigated.^{14,15}

Nitrogen-heterocyclic thiourea ligands can act as bridging units in some systems through thiourea sulfur and ring nitrogen atoms. Such coordination modes have been encountered especially in platinum group metal complexes.^{16–19} The nitrogen-heterocyclic thiourea ligands are also efficient ligands for coordination to a Cu(I) cation producing a variety of monomeric and polymeric structures.^{20,21} In addition, thioureas are widely recognized for their ability of

hydrogen-bond formation and consequently supramolecular network arrangement.²² Pyridine-thiourea derivatives also reveal great potential as ionophores for the detection of copper(II) ions in aqueous phase.²³

Interestingly, treating *N*⁷-aryl and *N*⁷-benzoyl functionalized *N*-(2-pyridyl)thiourea derivatives with copper(II) chloride resulted in a variety of coordination compounds where a [1,2,4]thiadiazolo[2,3-*a*]pyridin-4-ium cation was coordinated to the copper centre.^{24–26} It has been established that the *N*-(2-pyridyl)thiourea could easily be oxidized by copper(II) into the corresponding [1,2,4]thiadiazolo[2,3-*a*]pyridin-4-ium cation. These types of coordination compounds have been examined *in vitro* for their cytotoxic activity against human cancer cell lines showing promise in anticancer treatment.²⁶

Although reported to undergo oxidative cyclisation into 2-amino-[1,2,4]thiadiazolo[2,3-*a*]pyridin-4-ium cation on treatment with sulphuryl chloride,^{27,28} or bromine,^{27,29–31} to our knowledge the cyclisation of the parent unsubstituted *N*-(2-pyridyl)thiourea with CuCl_2 has not been studied yet.

Herein we report that the reaction of *N*-(2-pyridyl)thiourea with CuCl_2 in methanol solution affords four dif-

ferent crystalline products: small yellow crystals, $[\text{Cu}_2\text{Cl}_2(\mu\text{-Cl})_2(\text{L})_2]$ (**1**), a red polymeric complex, $[\text{Cu}_3\text{Cl}_8\text{L}_2]_n$ (**2**), a larger orange crystalline product with ionic structure, $\text{L}_2[\text{CuCl}_4]$ (**3**) and a colourless ionic compound LCl (**4**) ($\text{L} = 2\text{-amino-[1,2,4]thiadiazolo[2,3-}a\text{]pyridin-4-ium cation}$). The 2-amino-[1,2,4]thiadiazolo[2,3-*a*]pyridin-4-ium cation is the result of oxidative cyclization of *N*-(2-pyridyl)thiourea with copper(II). The structures of compounds **1–4** were determined by single-crystal X-ray diffraction analysis. The powder X-ray diffraction analysis was performed to analyse multicomponent products in the reaction mixture.

2. Experimental

General Procedure. *N*-(2-Pyridyl)thiourea and other reagents were purchased from commercial sources and were used as received. Proton NMR spectra were recorded at 500 MHz with a Bruker Avance III 500 spectrometer and referenced to $\text{Si}(\text{CH}_3)_4$ as an internal standard.

Synthesis. *N*-(2-pyridyl)thiourea (100 mg; 0.653 mmol) was dissolved in MeOH (10 mL). A few drops of Et_3N were added, followed by the addition of solid CuCl_2 (88 mg; 0.653 mmol). The resulting suspension was stirred for 40 min at room temperature. The undissolved residue

was filtered off and the clear green filtrate was kept at room temperature. After 4–5 days, slow evaporation of methanol from the filtrate afforded crystals of **1–4**. The relative yields were $1 > 3 > 2 > 4$. Small quantities of each of these compounds were separated from the mixture of products manually under microscope.

X-ray Crystallography. Crystal data and refinement parameters of compounds **1–4** are listed in Table 1. The X-ray intensity data were collected on a Nonius Kappa CCD diffractometer equipped with graphite-monochromated Mo K α radiation ($\lambda = 0.71073 \text{ \AA}$) at room temperature. The data were processed using DENZO.³² The structures were solved by direct methods using SHELXS-2013/1³³ or SIR-2014³⁴ and refined against F^2 on all data by a full-matrix least-squares procedure with SHELXL-2016/4.³³ All non-hydrogen atoms were refined anisotropically. All hydrogen atoms bonded to carbon were included in the model at geometrically calculated positions and refined using a riding model. The nitrogen bonded hydrogen atoms were located in the difference map and refined with the distance restraints (DFIX) with $d(\text{N-H}) = 0.86 \text{ \AA}$ and with $U_{\text{iso}}(\text{H}) = 1.2U_{\text{eq}}(\text{N})$. Finally, the three residual peaks in the structure of compound **2** higher than 1 e\AA^{-3} were observed near to the Cu or Cl atoms, with no chemical meaning.

X-Ray powder diffraction data were collected using a PANalytical X'Pert PRO MPD diffractometer with $\theta\text{-}2\theta$

Table 1. Crystal data and structure refinement details for **1–4**.

	1	2	3	4
formula	$\text{C}_{12}\text{H}_{12}\text{Cl}_4\text{Cu}_2\text{N}_6\text{S}_2$	$\text{C}_{12}\text{H}_{12}\text{Cl}_8\text{Cu}_3\text{N}_6\text{S}_2$	$\text{C}_{12}\text{H}_{12}\text{Cl}_4\text{CuN}_6\text{S}_2$	$\text{C}_6\text{H}_6\text{ClN}_3\text{S}$
Fw (g mol ⁻¹)	573.28	778.62	509.74	187.65
crystal size (mm)	$0.10 \times 0.08 \times 0.05$	$0.10 \times 0.05 \times 0.03$	$0.25 \times 0.20 \times 0.05$	$0.40 \times 0.08 \times 0.05$
crystal color	yellow	red	orange	colorless
crystal system	monoclinic	monoclinic	triclinic	triclinic
space group	<i>C</i> 2/ <i>c</i>	<i>C</i> 2/ <i>c</i>	<i>P</i> -1	<i>P</i> -1
<i>a</i> (Å)	17.1791(9)	14.8897(4)	8.5710(2)	5.2892(2)
<i>b</i> (Å)	7.1000(5)	13.1658(3)	10.4873(4)	7.4109(5)
<i>c</i> (Å)	15.5496(8)	12.0204(3)	11.9667(5)	10.2184(6)
α (°)	90	90	110.638(2)	81.224(3)
β (°)	95.548(4)	94.174(2)	106.838(2)	80.666(3)
γ (°)	90	90	93.453(2)	82.732(3)
<i>V</i> (Å ³)	1887.72(19)	2350.17(10)	947.51(6)	388.48(4)
<i>Z</i>	4	4	2	2
calcd density (g cm ⁻³)	2.017	2.201	1.787	1.604
<i>F</i> (000)	1136	1524	510	192
no. of collected reflns	4034	5130	6643	2807
no. of independent reflns	2127	2655	4219	1753
R_{int}	0.0320	0.0208	0.0222	0.0191
no. of reflns observed	1535	2156	3257	1403
no. of parameters	124	149	238	106
$R[I > 2\sigma(I)]^a$	0.0440	0.0446	0.0354	0.0314
wR_2 (all data) ^b	0.1025	0.1252	0.0812	0.0832
Goof, S^c	1.095	1.045	1.067	1.053
Largest diff. peak/hole (e Å ⁻³)	+0.42/-0.52	+2.36/-0.691	+0.34/-0.35	+0.22/-0.26

^a $R = \sum |F_o| - |F_c| / \sum |F_o|$. ^b $wR_2 = \{\sum [w(F_o^2 - F_c^2)^2] / \sum [w(F_o^2)^2]\}^{1/2}$. ^c $S = \{\sum [w(F_o^2 - F_c^2)^2] / (n-p)\}^{1/2}$ where *n* is the number of reflections and *p* is the total number of parameters refined.

reflection geometry, primary side Johansson type monochromator and Cu K α_1 radiation ($\lambda = 1.54059 \text{ \AA}$). The ambient temperature XRD spectrum of a sample was acquired from 2θ angles of 5° to 80° in steps of 0.034° with integration time of 100 seconds using a 128 rtms channel detector. Simulated powder diffraction pattern were calculated from single crystal structural data by Mercury³⁵ program.

3. Results and Discussion

Synthetic Aspects. The reaction between equimolar amounts of *N*-(2-pyridyl)thiourea and CuCl₂ was performed in methanol solution in the presence of a small quantity of Et₃N. Four different crystalline products were obtained after evaporation of solvent from the clear green solution. Figure 1 shows a photograph of the crystalline products: yellow (1), red (2), orange (3) and colourless crystals (4). Samples of each type could be manually collected and characterized by ¹H NMR spectroscopy and X-ray diffraction analyses. Small quantities of an amorphous green deposit were also found at the bottom of the vial but we are unable to characterize it.

From the crystal structure analyses it was evident that in all cases the *N*-(2-pyridyl)thiourea starting compound underwent oxidative cyclization into a 2-amino-[1,2,4]thiadiazolo[2,3-*a*]pyridin-4-ium cation (L) as shown in Scheme 1. A part of CuCl₂, added to the reaction

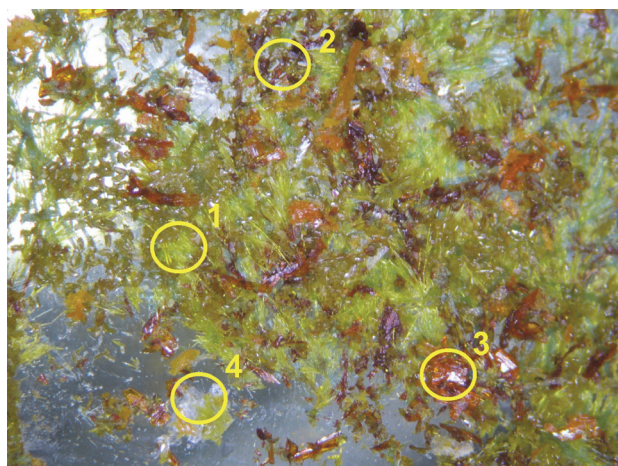
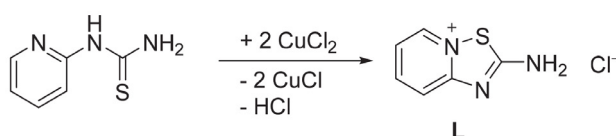


Figure 1. Photography of the bottom of vial containing the products of reaction between *N*-(2-pyridyl)thiourea and CuCl₂: yellow (1), red (2), orange (3) and colourless crystals (4).



Scheme 1. Oxidative cyclization of *N*-(2-pyridyl)thiourea with CuCl₂ forming 2-amino-[1,2,4]thiadiazolo[2,3-*a*]pyridin-4-ium cation (L).

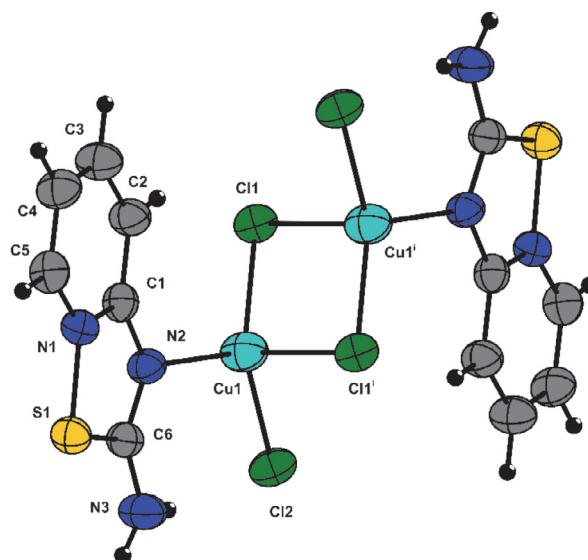


Figure 2. Molecular structure of **1** showing the atom-labeling scheme. The ellipsoids are shown at a probability level of 50%. Symmetry code: (i) $-x+1/2, -y+3/2, -z+1$.

Table 2. Selected bond lengths (Å) and angles (°) of compounds **1–4**.^a

1			
Cu1–Cl1	2.2837(12)	Cl1–Cu1–Cl2	116.92(4)
Cu1–Cl1 ⁱ	2.5352(13)	Cl1–Cu1–Cl1 ⁱ	104.50(4)
Cu1–Cl2	2.3072(12)	Cl1–Cu1–N2	116.26(10)
Cu1–N2	2.069(3)	Cl2–Cu1–N2	115.66(10)
N1–S1	1.731(3)	Cu1–Cl1–Cu1 ⁱ	75.50(4)
S1–C6	1.762(4)	N1–S1–C6	86.92(18)
2			
Cu1–Cl1	2.2799(9)	Cl1–Cu1–Cl2	91.16(4)
Cu1–Cl2	2.2985(9)	Cl1–Cu1–Cl3	173.28(3)
Cu1–Cl3	2.2931(9)	Cl1–Cu1–Cl4	91.22(4)
Cu1–Cl4	2.3076(9)	Cl1–Cu1–Cl5	85.11(3)
Cu1–Cl5	2.946(1)	Cl1–Cu1–N2	95.52(8)
Cu1–N2	2.546(3)	Cl1–Cu2–Cl1 ⁱⁱ	180.00(4)
Cu2–Cl1	3.005(1)	Cl1–Cu2–Cl4 ⁱⁱ	105.35(3)
Cu2–Cl4	2.3290(9)	Cu1–Cl1–Cu2	74.47(3)
Cu2–Cl5	2.2672(9)	Cu1–Cl4–Cu2	88.97(3)
N1–S1	1.710(3)	Cu1–Cl5–Cu2	75.87(3)
S1–C6	1.756(4)	N1–S1–C6	88.21(17)
3			
Cu1–Cl1	2.2932(8)	Cl1–Cu1–Cl2	99.32(3)
Cu1–Cl2	2.2184(8)	Cl1–Cu1–Cl3	122.87(3)
Cu1–Cl3	2.2567(7)	Cl1–Cu1–Cl4	99.55(3)
Cu1–Cl4	2.2300(8)	Cl2–Cu1–Cl3	98.65(3)
N1–S1	1.720(2)	Cl2–Cu1–Cl4	139.35(3)
S1–C6	1.761(3)	N1–S1–C6	86.95(12)
4			
N1–S1	1.7293(15)	N1–S1–C6	86.38(8)
S1–C6	1.7632(17)	N3–C6–S1	121.23(14)

^a Symmetry transformations used to generate equivalent atoms: (i) $-x+1/2, -y+3/2, -z+1$; (ii) $-x+1/2, -y+1/2, -z$.

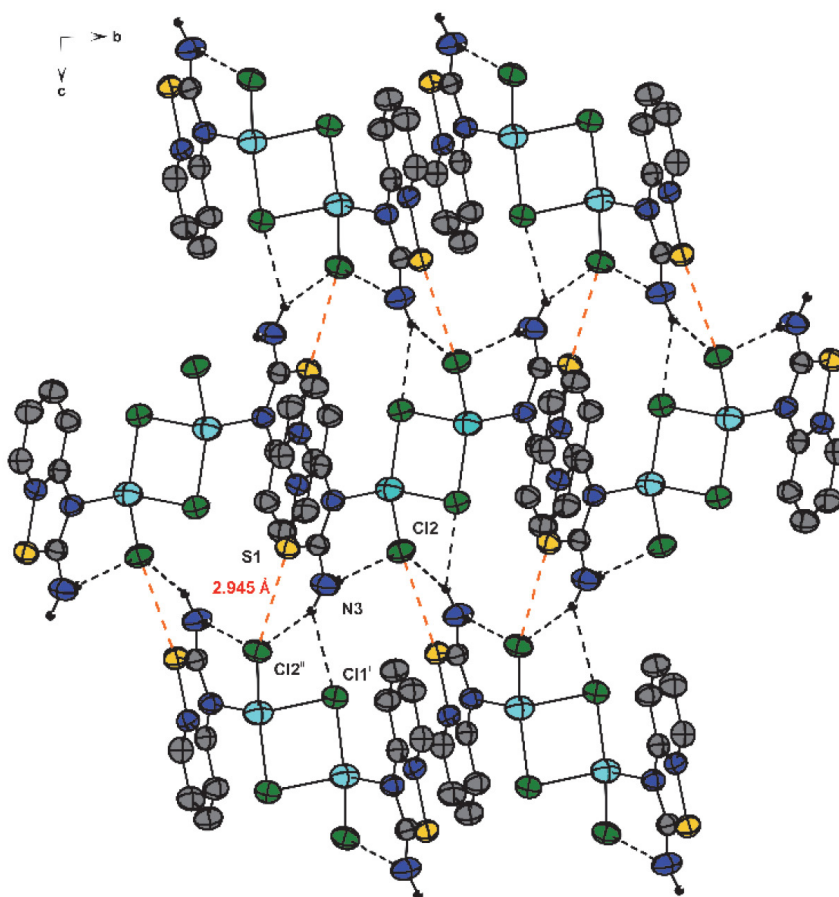


Figure 3. Layer formation in **1** through N–H...Cl hydrogen bonds and S...Cl contacts. The hydrogen atoms on aromatic rings have been removed for clarity. The ellipsoids are shown at a probability level of 50%. Symmetry codes: (i) $x, -y+1, z+1/2$; (ii) $-x+1/2, y-1/2, -z+3/2$.

Table 3. Hydrogen bonding geometry for **1**, **2**, **3** and **4**.

D – H ... A	d(D – H)/ Å	d(H ... A)/ Å	d(D ... A)/ Å	$\angle(\text{DHA})/^\circ$	Symmetry transformation for acceptors
1					
N3–H2N...Cl1	0.86(2)	2.78(5)	3.258(4)	116(4)	$x, -y+1, z+1/2$
N3–H1N...Cl2	0.86(2)	2.57(3)	3.391(4)	159(5)	
N3–H2N...Cl2	0.86(2)	2.40(3)	3.160(4)	148(5)	$-x+1/2, y-1/2, -z+3/2$
2					
N3–H1N...Cl1	0.848(19)	2.64(3)	3.398(4)	150(5)	
N3–H2N...Cl1	0.85(2)	2.63(4)	3.273(4)	134(5)	$x, -y, z+1/2$
N3–H2N...Cl5	0.85(2)	2.82(4)	3.533(4)	142(5)	$x, -y, z+1/2$
3					
N3–H1N...N5	0.855(18)	2.265(18)	3.119(3)	176(3)	
N3–H2N...Cl4	0.861(18)	2.48(2)	3.250(2)	149(3)	
N6–H3N...Cl3	0.849(18)	2.416(19)	3.254(3)	169(3)	
N6–H4N...Cl1	0.853(18)	2.47(2)	3.234(3)	149(3)	$-x+1, -y+1, -z+2$
4					
N3–H1N...Cl1	0.865(16)	2.27(2)	3.0319(18)	147(2)	
N3–H2N...N2	0.860(16)	2.286(18)	3.123(2)	164(2)	$-x+2, -y+1, -z+2$

mixture was reduced into copper(I) during oxidative cyclization and got involved into the coordination. Triethyl-

amine assisted deprotonation of the thiamine group and neutralized the reaction mixture.

X-ray analysis of complex 1. The molecular structure of **1** shows the dinuclear complex to be a bis-chlorido-bridged copper(I) compound (Fig. 2 and Fig. S1). Selected bond lengths and angles are summarized in Table 2. The coordination polyhedron of each copper atom in the structure of complex **1** is a distorted tetrahedron. Each copper atom is coordinated by ligand **L**, one terminal and two bridging chlorine atoms. One bridging Cu–Cl bonding distance (2.284 Å) is shorter whereas the other (2.535 Å) is longer as compared to the terminal Cu–Cl bonding distance (2.307 Å). The Cu–N bond distance of 2.069 Å is slightly longer than the corresponding Cu(II)–N bond distance in similar compounds (from 1.988 to 1.996 Å).²⁶ The Cu...Cu separation of 2.957 Å suggest a narrow Cu–Cl–Cu angle in **1**. Discrete dinuclear units are connected into a 2D network parallel to the *bc* plane by N–H...Cl hydrogen bonds (Fig. 3, Table 3) and by S...Cl interactions of 2.945 Å. The 2D layers are then π – π stacked with a centroid-to-centroid separation distance between two pyridine rings of 3.731 Å into 3D array (Fig. 4).

X-ray analysis of complex 2. The structure of **2** features a linear homonuclear Cu(II) chloride polymer in which the $\text{Cu}_3\text{Cl}_8\text{L}_2$ is the repeating unit (Fig. 5 and Fig. S2). Selected bond lengths and angles are given in Table 2. All chlorine atoms in these infinite chains are in the bridging positions. The coordination geometry around all copper atoms can be described as a distorted octahedron (Fig.

5). One type of copper atoms is coordinated by six chlorine atoms whereas the other is surrounded by five chlorine atoms and one **L** ligand. The Cu–N distance to the ligand **L** is 2.546 Å and is significantly longer than in the case of complex **1**. The Cu–Cl distances are in the range from normal 2.267 Å to very long Cu...Cl interaction of 3.005 Å. The structures with such elongated octahedra and very long Cu...Cl interaction can be found in the literature.³⁶ The elongated Cu...Cl and Cu...N interactions likely result from Jahn-Teller distortion. Two different Cu...Cu separations of 3.25 Å and 3.36 Å are longer than in compound **1** where copper is in +1 oxidation state. All the chlorido bridged copper atoms form a *zig-zag* chain, with the angles between the neighboring Cu atoms of 139° and 180°. The whole structure is stabilized by the N–H...Cl hydrogen bonding interactions, π – π stacking (3.878 Å) and by S...Cl interactions of 3.112 Å constructing a 3D network (Fig. 6, Table 3).

X-ray analysis of compound 3. The asymmetric unit of **3** consists of one $[\text{CuCl}_4]^{2-}$ anion and two **L** cations (Fig. S3). The packing of the structural units is depicted in Fig. 7. The coordination environment of the copper atom is tetrahedral with Cu–Cl distances ranging from 2.218 Å to 2.293 Å (Table 2), which is typical for tetrahedral $[\text{CuCl}_4]^{2-}$ ions. The cationic ligand **L** does not coordinate to the Cu atom in the structure of compound **3**. Four cations and two anions are connected by N–H...Cl and N–H...N hydrogen bonds (Table 3) and also by S...Cl inter-

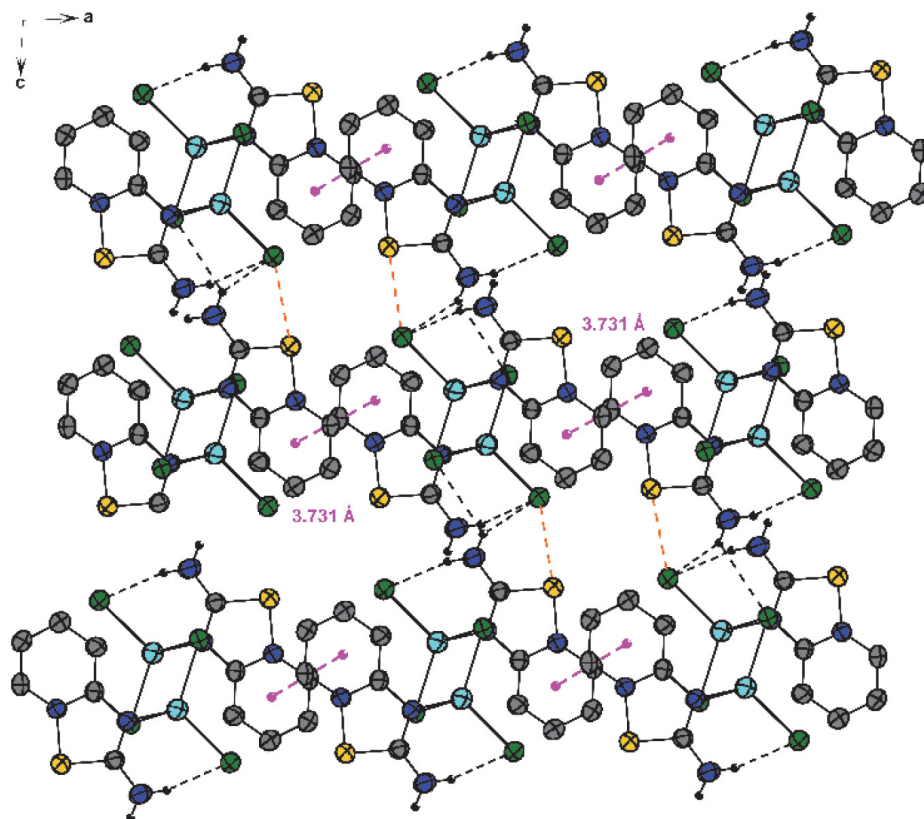


Figure 4. Fragment of the crystal packing of **1** with π – π stacking between pyridine rings. The ellipsoids are shown at a probability level of 50%.

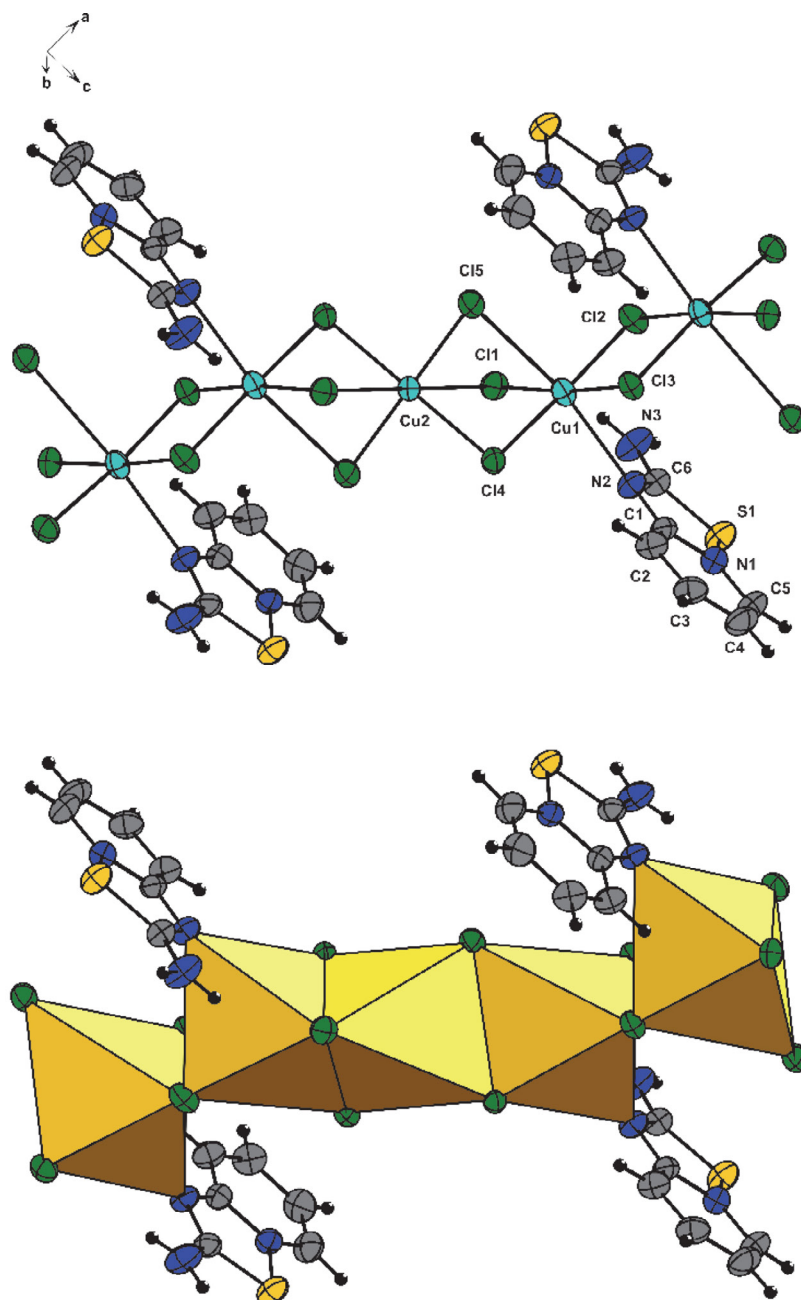


Figure 5. Molecular structure of **2** showing the atom-labeling scheme (above) and distorted octahedra representation (below). The ellipsoids are shown at a probability level of 50%.

actions into a discrete unit in the crystal structure. The S...Cl interaction distances are of two types, 3.029 and 3.113 Å, respectively. These units are then connected by π - π stacking interactions between the fused thiadiazole rings into chains along the *c*-axis with an interring distance of 3.673 Å (Fig. 8).

X-ray analysis of compound 4. The colorless crystals are an ionic phase without copper incorporated into the structure (Table 2 and Fig. S4). The reaction of formation of this ionic compound **4** is depicted in Scheme 1. Two cationic ligands **L** are connected by N-H...N hydro-

gen bonds into dimeric species (Fig. 9). The chloride anion is acceptor of a N-H...Cl hydrogen bond from the amino group of the ligand **L** (Table 3). These dimeric species are also stabilized by S...Cl interaction of 2.868 Å. In addition, the chloride anion is involved in other weak C-H...Cl hydrogen bonding interactions to form the 2D network in the crystal structure.

NMR spectra. The ^1H NMR spectra of compounds **1**, **2** and **3** recorded in DMSO- d_6 solutions (Figures S5–S7) are nearly identical indicating ligand **L** dissociation from the copper center in the solution. In comparison to the

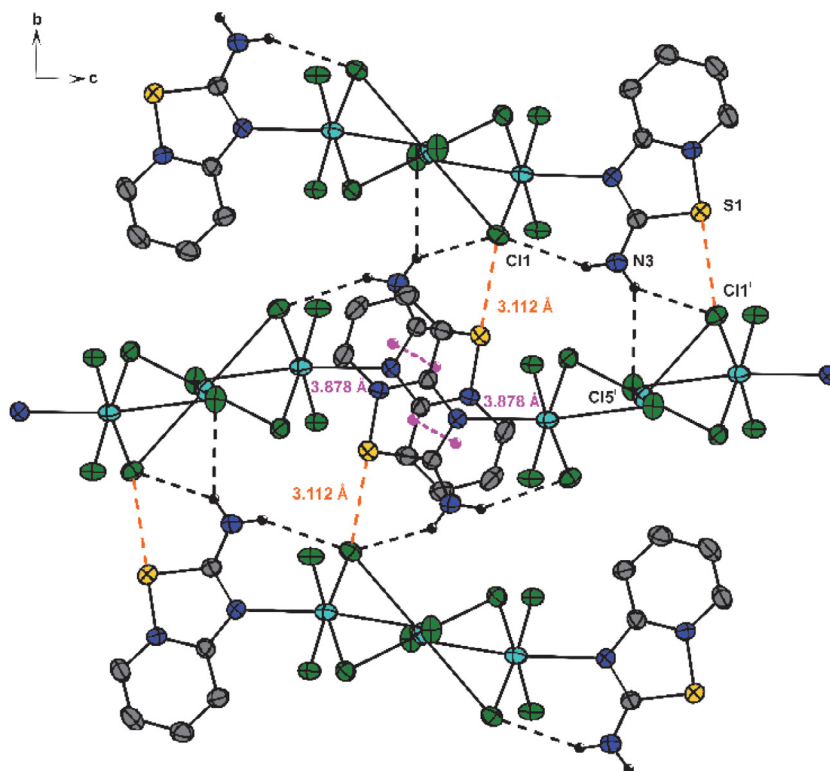


Figure 6. Fragment of the crystal packing in **2** with N–H...Cl hydrogen bonds, π – π stacking and S...Cl contacts. The hydrogen atoms on aromatic rings have been removed for clarity. The ellipsoids are shown at a probability level of 50%. Symmetry code: (i) $x, -y, z+1/2$.

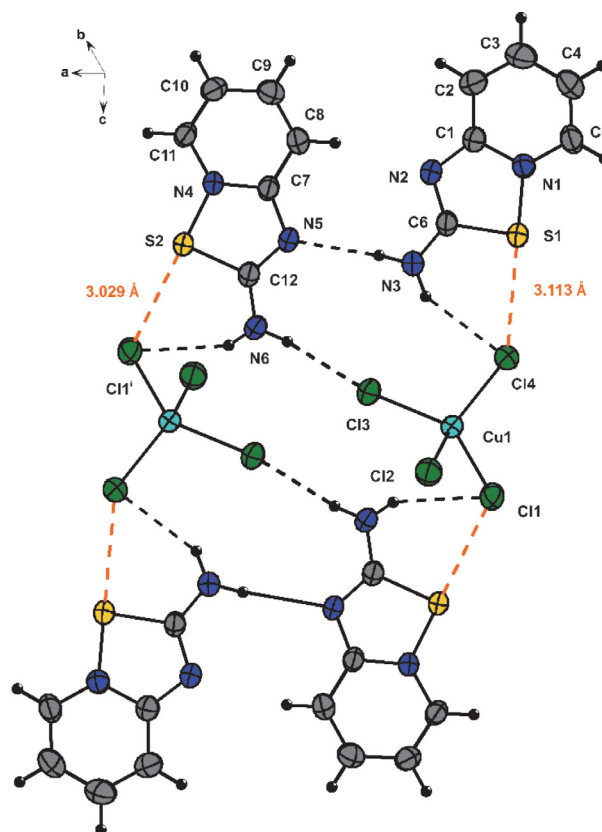


Figure 7. Fragment of crystal packing and the atom-labeling scheme of **3** with N–H...Cl and N–H...N hydrogen bonds and S...Cl interactions. The ellipsoids are shown at a probability level of 50%. Symmetry code: (i) $-x+1, -y+1, -z+2$.

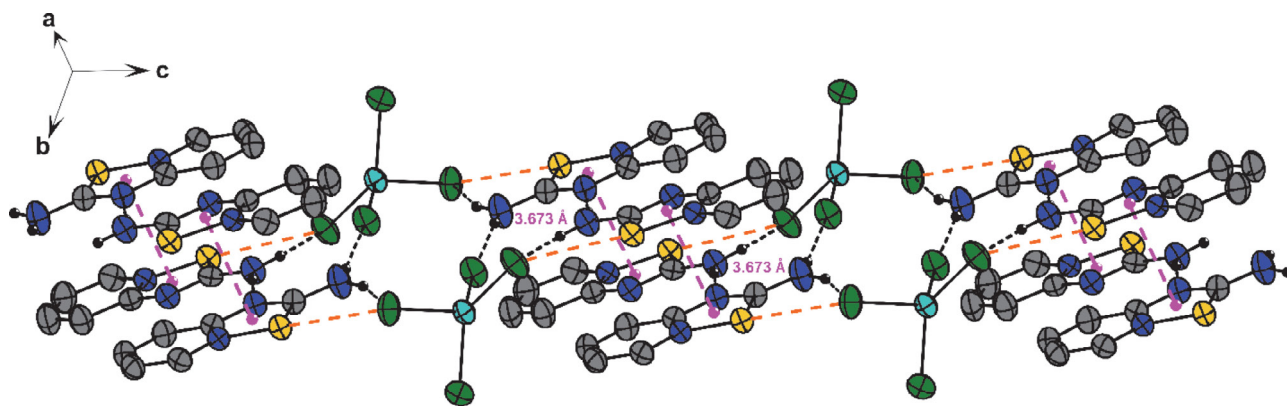


Figure 8. Fragment of crystal packing of 3 with π - π stacking between thiadiazole rings. The ellipsoids are shown at a probability level of 50%.

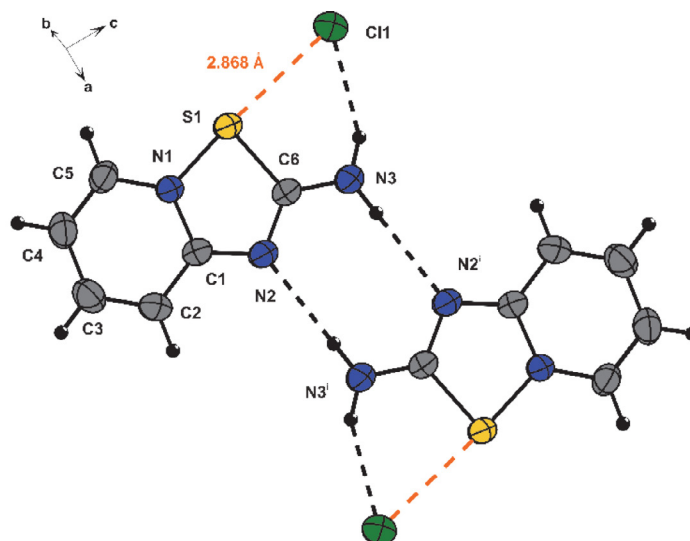


Figure 9. Fragment of crystal packing and the atom-labeling scheme of 3 with N-H...Cl and N-H...N hydrogen bonds and S...Cl interactions. The ellipsoids are shown at a probability level of 50%. Symmetry code: (i) $-x+2, -y+1, -z+2$.

starting *N*-(2-pyridyl)thiourea (Figure S8), the spectra of compounds 1–3 lack broad N–H resonance at δ 8.90 ppm (Fig. 10). The presence of 2-amino-[1,2,4]thiadiazolo[2,3-*a*]pyridin-4-ium cation is confirmed by a significant downfield shift of the electron-deficient fused pyridine protons resonating at δ 9.05 (d), 8.06 (dd), 7.70 (d)

7.33 (dd) ppm as compared to the *N*-(2-pyridyl)thiourea (δ 8.24 (d), 7.77 (dd), 7.16 (d), 7.05 (dd) ppm) and upfield shift for amino NH_2 hydrogen atoms (from 10.59 (s), 10.53 (s) ppm to 9.70 (s), 9.48 (s) ppm). The ^1H NMR chemical shifts of ligand L are in agreement with those for the substituted [1,2,4]thiadiazolo[2,3-*a*]pyridin-4-ium cations reported in the literature.^{25,26}

Powder diffraction X-ray analysis. The product of the reaction was characterized by X-ray powder diffraction. There is clear evidence that the sample is a mixture of compounds 1–4 (Fig. 11). No other crystalline phases were additionally present since all diffraction peaks in the powder pattern of the sample can be contributed to compounds 1–4.

4. Conclusion

In summary, four different crystalline complexes have been found as products of the reaction between

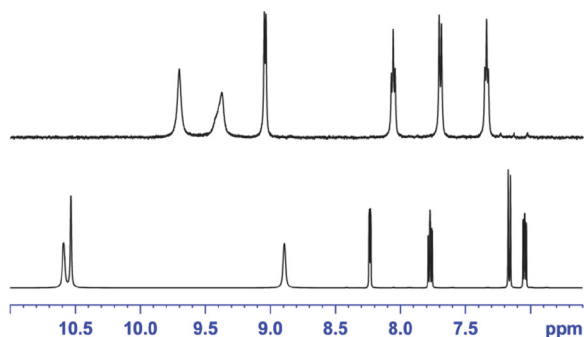


Figure 10. Selected parts of ^1H NMR spectra of compound 2 (above) and *N*-(2-pyridyl)thiourea (below).

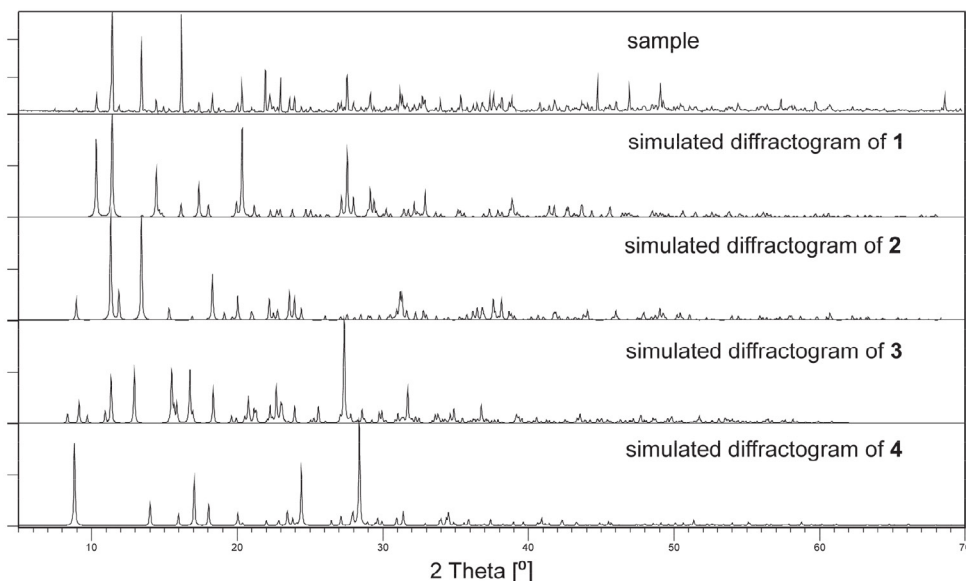


Figure 11. Comparison of the measured powder diffraction pattern of the reaction product and the simulated diffraction patterns of **1–4**. Intensities of diffracted x-rays are given in arbitrary units.

N-(2-pyridyl)thiourea and CuCl_2 . Oxidative cyclization of *N*-(2-pyridyl)thiourea occurred with copper(II) chloride as an oxidant affording thiadiazolopyridinium cation as planar ligand. The complexes consist of a dimeric dinuclear unit (**1**), polymeric chains (**2**) and ionic (**3**) compounds. Copper(I) ions, which are a product of reduction of Cu(II) to Cu(I) and concomitant oxidation of *N*-(2-pyridyl)thiourea, are incorporated in complex **1**. Complexes **2** and **3** contain copper(II) while the ionic compound **4** contains a cationic ligand **L** with chlorine counter ion. The crystal structure determinations have established the existence of N–H...Cl hydrogen bonding interactions in all crystal structures. The remarkable feature of the **1–4** compounds is that there are S...Cl interactions involved in the crystal packing. Intermolecular or interionic S...Cl contacts with distances from 2.87 to 3.11 Å are significantly shorter than the corresponding van der Waals radii sum of 3.65 Å.³⁷ The short S...Cl contacts are now widely interpreted as chalcogen bonds.^{38–41} The X-ray diffraction analysis compared the experimental powder diffraction pattern of the product of the reaction with the simulated diffraction patterns for all compounds **1–4** obtained from the single-crystal structure analysis.

Supplementary Material

The Supporting Information is available: ORTEP view of compounds **1–4**, ¹H NMR spectra of compounds **1–3** and *N*-(2-pyridyl)thiourea.

CCDC 1812471–1812474 contain the supplementary crystallographic data for this paper. This data can be obtained free of charge via www.ccdc.cam.ac.uk/data_request/cif, or by emailing data_request@ccdc.cam.ac.uk, or by contacting The Cambridge Crystallographic Data Cen-

tre, 12 Union Road, Cambridge CB2 1EZ, UK; fax: +44 1223 336033.

Acknowledgements

This work was supported by the Slovenian Research Agency (Grants: P1-0175 and P1-0230). Authors also thank to Dr. Marta Počkaj for her extremely helpful comments on powder diffraction analysis.

5. References

1. E. W. Ainscough, A. M. Brodie, *Coord. Chem. Rev.* **1978**, *27*, 59–86. DOI:10.1016/S0010-8545(00)80353-7
2. R. G. Vranka, E. L. Amma, *J. Am. Chem. Soc.* **1966**, *88*, 4270–4271. DOI:10.1021/ja00970a036
3. A. G. Gash, E. H. Griffith, W. A. Spofford, III, E. L. Amma, *J. Chem. Soc., Chem. Commun.* **1973**, 256–257. DOI:10.1039/c39730000256
4. I. F. Taylor, Jr., M. S. Weininger, E. L. Amma, *Inorg. Chem.* **1974**, *13*, 2835–2842. DOI:10.1021/ic50142a014
5. E. H. Griffith, G. W. Hunt, E. L. Amma, *J. Chem. Soc., Chem. Commun.* **1976**, 432–433. DOI:10.1039/C39760000432
6. J. P. Declercq, R. Kamara, C. Moreaux, J. M. Dereppe, G. Germain, M. Van Meerssche, *Acta Cryst.* **1978**, *B34*, 1036–1037. DOI:10.1107/S0567740878004793
7. R. C. Bott, G. A. Bowmaker, C. A. Davis, G. A. Hope, B. E. Jones, *Inorg. Chem.* **1998**, *37*, 651–657. DOI:10.1021/ic970910q
8. O. E. Piro, R. C. V. Piatti, A. E. Bolzán, R. C. Salvarezza, A. J. Arvia, *Acta Cryst.* **2000**, *B56*, 993–997. DOI:10.1107/S0108768100008028
9. P. Bombicz, I. Mutikainen, M. Krunks, T. Leskelä, J. Madarász,

- L. Niinistö, *Inorg. Chim. Acta* **2004**, *357*, 513–525.
DOI:10.1016/j.ica.2003.08.019
10. S. Athimoolam, J. Kumar, V. Ramakrishnan, R. K. Rajaram, *Acta Cryst.* **2005**, *E61*, m2014–m2017.
DOI:10.1107/S1600536805028588
11. G. A. Bowmaker, J. V. Hanna, C. Pakawatchai, B. W. Skelton, Y. Thanyasirikul, A. H. White, *Inorg. Chem.* **2009**, *48*, 350–368.
DOI:10.1021/ic801310r
12. H. Zouihri, *Acta Cryst.* **2012**, *E68*, m260–m261.
DOI:10.1107/S1600536812004448
13. E. A. H. Griffith, W. A. Spofford, III, E. L. Amma, *Inorg. Chem.* **1978**, *17*, 1913–1917. DOI:10.1021/ic50185a043
14. D. A. Zatko, B. Kratochvil, *Anal. Chem.* **1968**, *40*, 2120–2123.
DOI:10.1021/ac50158a031
15. C. J. Doona, D. M. Stanbury, *Inorg. Chem.* **1996**, *35*, 3210–3216. DOI:10.1021/ic9502077
16. M. L. Soriano, J. T. Lenthall, K. M. Anderson, S. J. Smith, J. W. Steed, *Chem. Eur. J.* **2010**, *16*, 10818–10831.
DOI:10.1002/chem.201001354
17. J. G. Małeckı, J. Nycz, *Polyhedron* **2013**, *55*, 49–56.
DOI:10.1016/j.poly.2013.02.056
18. M. Kalidasan, R. Nagarajaparakash, S. Forbes, Y. Mozharivskyj, K. M. Rao, *Z. Anorg. Allg. Chem.* **2015**, *641*, 715–723.
DOI:10.1002/zaac.201400491
19. M. Kalidasan, R. Nagarajaparakash, K. M. Rao, *Transition Met. Chem.* **2015**, *40*, 531–539.
DOI:10.1007/s11243-015-9946-x
20. Y. Fan, H. Lu, H. Hou, Z. Zhou, Q. Zhao, L. Zhang, F. Cheng, *J. Coord. Chem.* **2000**, *50*, 65–72.
DOI:10.1080/00958970008054925
21. A. Saxena, E. C. Dugan, J. Liaw, M. D. Dembo, R. D. Pike, *Polyhedron* **2009**, *28*, 4017–4031.
DOI:10.1016/j.poly.2009.08.023
22. A. Saxena, R. D. Pike, *J. Chem. Crystallogr.* **2007**, *37*, 755–764.
DOI:10.1007/s10870-007-9246-1
23. W. M. Khairul, H. M. Zuki, M. F. A. Hasan, A. I. Daud, *Procedia Chem.* **2016**, *20*, 105–114.
DOI:10.1016/j.proche.2016.07.019
24. D.-J. Che, G. Li, Z. Yu, D.-P. Zou, C.-X. Du, *Inorg. Chem. Commun.* **2000**, *3*, 537–540.
DOI:10.1016/S1387-7003(00)00115-5
25. G. Li, D.-J. Che, Z.-F. Li, Y. Zhu, D.-P. Zou, *New J. Chem.* **2002**, *26*, 1629–1633. DOI:10.1039/B206257G
26. F. Adhami, M. Safavi, M. Ehsani, S. K. Ardestani, F. Emmerling, F. Simyari, *Daton Trans.* **2014**, *43*, 7945–7957.
DOI:10.1039/C3DT52905C
27. R. L. N. Harris, *Aust. J. Chem.* **1972**, *25*, 993–1001.
DOI:10.1071/CH9720985
28. A. Castro, A. Martinez, *J. Heterocyclic. Chem.* **1999**, *36*, 991–995. DOI:10.1002/jhet.5570360427
29. B. Koren, B. Stanovnik, M. Tisler, *Org. Prep. Proced. Int.* **1975**, *7*, 55–59. DOI:10.1080/00304947509355570
30. I. Leban, *Acta Cryst.* **1976**, *B32*, 1601–1604.
DOI:10.1107/S0567740876005980
31. G. Barnikow, J. Bödeker, *J. Prakt. Chem.* **1971**, *313*, 1148–1154. DOI:10.1002/prac.19713130622
32. Z. Otwinowski, W. Minor, *Methods Enzymol.* **1997**, *276*, 307–326. DOI:10.1016/S0076-6879(97)76066-X
33. G. M. Sheldrick, *Acta. Crystallogr.* **2015**, *C71*, 3–8.
DOI:10.1107/S0108767307043930
34. M. C. Burla, R. Caliandro, B. Carrozzini, G. L. Casciarano, C. Cuocci, C. Giacovazzo, M. Mallamo, A. Mazzone, G. Polidori, *J. Appl. Cryst.* **2015**, *48*, 306–309.
DOI:10.1107/S1600576715001132
35. C. F. Macrae, I. Sovago, S. J. Cottrell, P. T. A. Galek, P. McCabe, E. Pidcock, M. Platings, G. P. Shields, J. S. Stevens, M. Towler, P. A. Wood, *J. Appl. Cryst.* **2020**, *53*, 226–235.
DOI:10.1107/S1600576719014092
36. Y. Fujii, Z. Wang, R. D. Willett, W. Zhang, C. P. Landee, *Inorg. Chem.* **1995**, *34*, 2870–2874. DOI:10.1021/ic00115a013
37. L. Pauling, *The Nature of the Chemical Bond*; Cornell University Press, Ithaca, 1960.
38. D. J. Pascoe, K. B. Ling, S. L. Cockroft, *J. Am. Chem. Soc.* **2017**, *139*, 15160–15167. DOI:10.1021/jacs.7b08511
39. K. T. Mahmudov, M. N. Kopylovich, M. F. C. Guedes da Silva, A. J. L. Pombeiro, *Dalton Trans.* **2017**, *46*, 10121–10138.
DOI:10.1039/C7DT01685A
40. E. S. Yandanova, D. M. Ivanov, M. L. Kuznetsov, A. G. Starikov, G. L. Starova, V. Yu. Kukushkin, *Cryst. Growth Des.* **2016**, *16*, 2979–2987. DOI:10.1021/acs.cgd.6b00346
41. W. Wang, B. Ji, Y. Zhang, *J. Phys. Chem. A* **2009**, *113*, 8132–8135. DOI:10.1021/jp904128b

Povzetek

Pri reakciji med *N*-(2-piridil)tiosečnino in CuCl_2 v metanolu smo dobili štiri različne kristalinične produkte: rumene dimerne kristale, $[\text{Cu}_2\text{Cl}_2(\mu\text{-Cl})_2(\text{L})_2]$ (**1**), rdeč polimerni kompleks, $[\text{Cu}_3\text{Cl}_8\text{L}_2]_n$ (**2**), oranžni kristalinični product z ionsko zgradbo, $\text{L}_2[\text{CuCl}_4]$ (**3**), in brezbarvno ionsko spojino, LCl (**4**). Pri tem je $\text{L} = 2\text{-amino-[1,2,4]tiadiazolo[2,3-}a\text{]piridin-4-ijev kation}$, ki je nastal v raztopini kot produkt oksidativne ciklizacije *N*-(2-piridil)tiosečnine. Kristalne strukture vseh kristaliničnih produktov so bile določene s pomočjo rentgenske strukturne analize. V spojini **1** je baker(I) ion, medtem ko je v spojinah **2** in **3** baker kolt centralni ion v oksidacijskem stanju +2. ^1H NMR spektri spojin **1–3** so identični in potrjujejo deprotonacijo tioamidne skupine *N*-(2-piridil)tiosečnine ter tvorbo tiadiazolopiridinijevega kationa v raztopini. V kristalnih strukturah so bile proučene tudi vodikove vezi in $\pi\text{-}\pi$ interakcije. Poleg teh interakcij pa spojine **1–4** vsebujejo tudi $\text{S}\cdots\text{Cl}$ interakcije, ki povezujejo komplekse v trodimenzionalne tvorbe. Primerjava izračunanih rentgenskih praškovnih difraktogramov s difraktogramom produkta po reakciji nakazuje na odsotnost drugih kristaliničnih primesi.



Except when otherwise noted, articles in this journal are published under the terms and conditions of the Creative Commons Attribution 4.0 International License